Robustness of a partially interdependent network formed of clustered networks

Shuai Shao,[1] Xuqing Huang,[1] H. Eugene Stanley,[1] and Shlomo Havlin[1,2]
[1]*Center for Polymer Studies and Department of Physics, Boston University, Boston, Massachusetts 02215, USA*
[2]*Minerva Center and Department of Physics, Bar-Ilan University, Ramat-Gan 52900, Israel*
(Received 26 October 2013; published 25 March 2014)

Clustering, or transitivity, a behavior observed in real-world networks, affects network structure and function. This property has been studied extensively, but most of this research has been limited to clustering in single networks. The effect of clustering on the robustness of coupled networks, on the other hand, has received much less attention. Only the case of a pair of fully coupled networks with clustering has recently received study. Here we generalize the study of clustering of a fully coupled pair of networks and apply it to a partially interdependent network of networks with clustering within the network components. We show, both analytically and numerically, how clustering within networks affects the percolation properties of interdependent networks, including the percolation threshold, the size of the giant component, and the critical coupling point at which the first-order phase transition changes to a second-order phase transition as the coupling between the networks is reduced. We study two types of clustering, one proposed by Newman [Phys. Rev. Lett. **103**, 058701 (2009)] in which the average degree is kept constant while the clustering is changed, and the other by Hackett *et al.* [Phys. Rev. E **83**, 056107 (2011)] in which the degree distribution is kept constant. The first type of clustering is studied both analytically and numerically, and the second is studied numerically.

DOI: 10.1103/PhysRevE.89.032812 PACS number(s): 89.75.Hc, 64.60.ah, 64.60.aq

I. INTRODUCTION

Complex networks are a useful approach to understanding the structure, stability, and function of complex systems [1–17]. Clustering, the propensity of two neighbors of the same node to be also neighbors of each other, has been observed in many real-world networks [1,18–20]. For example, in a social network, if B and C are friends of A, they have a high probability of also being each other's friends. The average of this probability over the whole network is called the clustering coefficient. Empirical studies show that in many real-world networks, e.g., the Internet, scientific collaboration networks, metabolic and protein networks, and movie actor networks, the measured clustering coefficient is of the order of 10%, significantly higher than that of random networks [4,21].

Many computational models have been proposed to generate the clustering coefficient in networks, but all have been limited to numerical analysis [22–26]. Newman recently developed an analytical approach that incorporates clustering into random graphs by extending the generating function method, a widely used analytical tool in network research [27]. He considered two properties for each node, single links and triangles, and constructed a joint distribution for both. The clustering coefficient can be tuned by changing the ratio between the average number of single links and triangles. This approach enables us to evaluate analytically many properties of the resulting networks, such as component size, emergence and size of a giant component, and other percolation properties.

Previous studies of clustering have focused on single network analysis, but real-world networks interact with and depend on other networks. In 2010 Buldyrev *et al.* [28] developed a theoretical framework for studying percolation in two fully interdependent networks and observed an unusual first-order (abrupt) percolation transition that differed from the known second-order (continuous) phase transition in a single network. Parshani *et al.* [29] generalized this framework to partially interdependent networks and found a change from a first-order to a second-order phase transition when the coupling strength was reduced below a critical value. Since 2010 there have been many studies of interdependent networks, sometimes called "networks of networks" [30–47]. With respect to percolation properties, the specific case in which interdependent nodes in the network of networks are treated as identical is the multiplex network. However, from a dynamical point of view, e.g., diffusion or transport, these two systems (interdependent and multiplex) could be very different [48–50]. Recently Huang *et al.* [51] developed an approach to site percolation on clustered networks and studied the robustness of a pair of *fully* interdependent networks with clustering within each network.

Here we generalize the framework of Huang *et al.* [51] and extend it (i) to the study of percolation in two *partially* interdependent networks with clustering within each network and (ii) to the study of a network of clustered networks (NON), i.e., a network consisting of more than two interdependent clustered networks. We study how clustering within the networks influences such percolation properties as the critical threshold p_c at which the giant component collapses, the sizes of the giant components ψ_∞ and ϕ_∞ in the two networks, the critical coupling q_c at which the first-order phase transition changes to a second-order phase transition, and the dynamics of cascading failure between two clustered networks. Simulation results agree well with theoretical results in all cases.

In Sec. V we also examine two joint distribution models for incorporating clustering into random graphs, i.e., (i) the model proposed by Newman [27], in which a double-Poisson distribution (see Sec. III) is assumed for the joint degree distribution, and the average degree is kept constant while the clustering is changed; and (ii) the clustering model developed by Hackett *et al.* [52], in which a different joint distribution keeps both the average degree and the degree distribution constant while the clustering is changed. We discuss the similarities and differences in the percolation properties of

the networks generated by these two distribution models. The model presented by Newman is studied both analytically and via simulations (Secs. III and IV), and the model presented by Hackett *et al*. is studied using only simulations (Sec. V).

II. THE MODEL

In our model we consider two networks A and B that have the same number of nodes N. Within each network the nodes are connected with joint degree distribution $P_A(s,t)$ and $P_B(s,t)$, which specifies the fraction of nodes connected to s single links and t triangles in networks A and B, respectively [27]. The generating functions [53,54] of the joint degree distributions are

$$\begin{aligned} G_{A0}(x,y) &= \sum_{s,t=0}^{\infty} P_A(s,t)x^s y^t, \\ G_{B0}(x,y) &= \sum_{s,t=0}^{\infty} P_B(s,t)x^s y^t. \end{aligned} \tag{1}$$

The conventional degree of a node is $k = s + 2t$, and the conventional degree distributions of the networks are

$$\begin{aligned} P_A(k) &= \sum_{s,t=0}^{\infty} P_A(s,t)\delta_{k,s+2t}, \\ P_B(k) &= \sum_{s,t=0}^{\infty} P_B(s,t)\delta_{k,s+2t}. \end{aligned} \tag{2}$$

The clustering coefficient is defined in Ref. [53] as

$$c \equiv \frac{3 \times (\text{number of triangles in network})}{\text{number of connected triples}} = \frac{3N_\Delta}{N_3}, \tag{3}$$

where $3N_\Delta \equiv N\sum_{st} tP(s,t)$ and $N_3 = N\sum_k \binom{k}{2}P(k)$.

Our initial attack is the random removal of a $(1-p)$ fraction of nodes from network A. The generating function of the resulting network is [51]

$$\begin{aligned} G'_{A0}(x,y) &\equiv G_{A0}(x,y,p) \\ &= G_{A0}[xp + 1 - p, p^2 y + 2xp(1-p) + (1-p)^2], \end{aligned} \tag{4}$$

and the fraction of nodes belonging to the giant component in the remaining network is

$$g_A(p) = 1 - G_{A0}(u, v^2, p), \tag{5}$$

where u, v satisfy

$$u = G_{Aw}(u, v^2, p), \quad v = G_{Ar}(u, v^2, p). \tag{6}$$

The functions $G_{Aw}(x,y,p)$ and $G_{Ar}(x,y,p)$ are defined as

$$\begin{aligned} G_{Aw}(x,y,p) &\equiv \frac{1}{\langle s'\rangle}\frac{\partial G_{A0}(x,y,p)}{\partial x}, \\ G_{Ar}(x,y,p) &\equiv \frac{1}{\langle t'\rangle}\frac{\partial G_{A0}(x,y,p)}{\partial y}, \end{aligned} \tag{7}$$

where $\langle s'\rangle = \frac{\partial G_{A0}(x,y,p)}{\partial x}|_{x=1,y=1}$ and $\langle t'\rangle = \frac{\partial G_{A0}(x,y,p)}{\partial y}|_{x=1,y=1}$. Similar equations hold for network B.

We next consider the interaction between clustered networks A and B [29]. Assume a q_A fraction of nodes in network A is dependent on nodes in network B and a q_B fraction of nodes in network B is dependent on nodes in network A. This means that if a node in network B upon which a node in network A depends fails, the corresponding node in network A will also fail, and vice versa. We also assume that a node from one network may be dependent on no more than one node from the other network and if a node i in network A is dependent on a node j in network B and j depends on a node l in network A, then $l = i$ (a no-feedback condition [45–47]). After n steps of cascading failures, ψ_n and ϕ_n are the fractions of nodes in the giant components of networks A and B, respectively. After the two-network system reaches stationarity, the sizes of giant components in the two networks are [29]

$$\psi_\infty = xg_A(x), \quad \phi_\infty = yg_B(y), \tag{8}$$

where the two variables x and y satisfy

$$\begin{aligned} x &= p\{1 - q_A[1 - g_B(y)]\}, \\ y &= 1 - q_B[1 - pg_A(x)]. \end{aligned} \tag{9}$$

III. THE DOUBLE-POISSON DISTRIBUTION

As an example, consider two Erdős-Rényi (ER) networks [55–57] with clustering, in which the number of single links s and triangles t of a node obey a double-Poisson distribution $P_{st} = e^{-\langle s\rangle}\frac{\langle s\rangle^s}{s!}e^{-\langle t\rangle}\frac{\langle t\rangle^t}{t!}$ (s and t follow a Poisson distribution independently) [27]. Here $\langle s\rangle$ and $\langle t\rangle$ are the average number of single links and triangles per node, respectively. Assuming that in network A $\langle s\rangle = \langle s\rangle_A$ and $\langle t\rangle = \langle t\rangle_A$, then the generating functions in Eq. (4) and Eq. (7) become

$$\begin{aligned} G_{A0}(x,y,p) &= G_{Aw}(x,y,p) = G_{Ar}(x,y,p) \\ &= e^{[\langle s\rangle_A p + 2p(1-p)\langle t\rangle_A](x-1) + \langle t\rangle_A p^2(y-1)}, \end{aligned} \tag{10}$$

and the same holds for network B. Denoting $f_A(x) = 1 - g_A(x)$ and $f_B(y) = 1 - g_B(y)$, we now have

$$\begin{aligned} f_A(x) &= \exp\{\langle t\rangle_A x^2[1 - f_A(x)]^2 - \langle k\rangle_A x[1 - f_A(x)]\}, \\ f_B(y) &= \exp\{\langle t\rangle_B y^2[1 - f_B(y)]^2 - \langle k\rangle_B y[1 - f_B(y)]\}, \end{aligned} \tag{11}$$

where $\langle k\rangle_A$ and $\langle k\rangle_B$ are the average degrees for networks A and B, respectively ($\langle k\rangle_A = \langle s\rangle_A + 2\langle t\rangle_A$, and $\langle k\rangle_B = \langle s\rangle_B + 2\langle t\rangle_B$). By combining Eqs. (9) and (11) and eliminating x and y, we obtain two transcendental equations for f_A and f_B:

$$\begin{aligned} f_A &= e^{\langle t\rangle_A p^2(1-f_A)^2(1-q_A f_B)^2 - \langle k\rangle_A p(1-f_A)(1-q_A f_B)}, \\ f_B &= e^{\langle t\rangle_B (1-f_B)^2\{1-q_B[1-p(1-f_A)]\}^2 - \langle k\rangle_B (1-f_B)\{1-q_B[1-p(1-f_A)]\}}. \end{aligned} \tag{12}$$

By substituting the parameter vector $(\langle k\rangle_A, \langle t\rangle_A, \langle k\rangle_B, \langle t\rangle_B, q_A, q_B, p)$, we can solve for f_A and f_B, and thus find the size of the giant components in network A, ψ_∞, and network B, ϕ_∞. By substituting the double-Poisson distribution into Eq. (3),

the clustering coefficients in the two networks become

$$c_A = \frac{2\langle t\rangle_A}{\langle k\rangle_A^2 + 2\langle t\rangle_A}, \qquad c_B = \frac{2\langle t\rangle_B}{\langle k\rangle_B^2 + 2\langle t\rangle_B}. \tag{13}$$

If we fix the other parameters and increase p, the fraction of nodes not removed in the initial attack, a phase transition occurs at a critical threshold p_c and a giant component appears. As we decrease the coupling strength q_A and q_B, the behavior of this phase transition will change from first-order to second-order. A first-order phase transition, denoted by I, corresponds to a scenario in which the size of one or both giant components in the two networks collapses discontinuously from a finite value to zero. If we plot f_A and f_B in Eqs. (12) in a two-dimensional graph, this corresponds to the scenario that two curves $f_A(f_B)$ and $f_B(f_A)$ are tangential with each other ($\frac{df_B(f_A)}{df_A}\frac{df_A(f_B)}{df_B} = 1$) [29]. By adding this condition into Eqs. (12), we can solve for $f_A = f_{A_I}$, $f_B = f_{B_I}$, and $p = p_I$. A second-order phase transition (denoted by II), corresponding to a scenario in which the size of one or both giant components decreases continuously to zero, is obtained by substituting $f_A \to 1$ or $f_B \to 1$ into Eqs. (12), which allows us to find $f_{A_{II}}$, $f_{B_{II}}$, and p_{II}. The critical coupling strength q_c is solved by making the conditions for both first-order and second-order phase transitions equal.

For the sake of simplicity, we now consider the symmetrical case, $\langle k\rangle = \langle k\rangle_A = \langle k\rangle_B$ and $c = c_A = c_B$. Figure 1 shows the size of the giant components in networks A and B for several clustering coefficients. In each graph the simulation

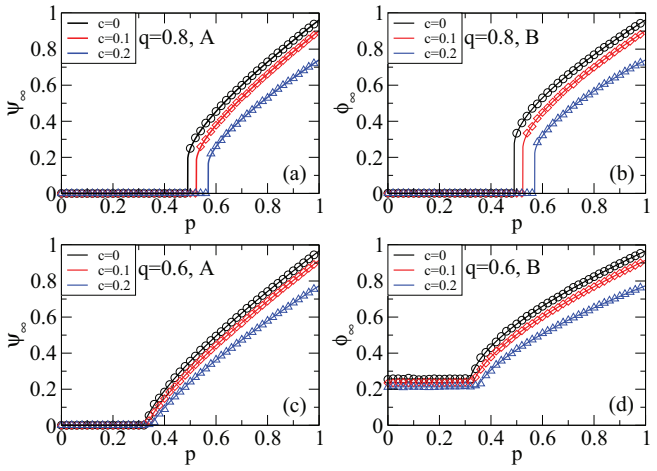

FIG. 1. (Color online) Size of giant components as a function of p for $\langle k\rangle = \langle k\rangle_A = \langle k\rangle_B = 4$, where solid lines are from theoretical predictions, Eqs. (12), and symbols are from simulations with network size $N = 10^5$. (a) and (b) For strong coupling ($q = 0.8$), the sizes of giant components in (a) network A and (b) network B change abruptly at some critical threshold p_c, showing a first-order phase transition behavior. (c) and (d) For weak coupling ($q = 0.6$), on the contrary, the behavior is continuous, i.e., second-order. Note that while (c) network A collapses (d) network B does not collapse, since the initial failures are in A and q is relatively small to cause collapse of network B. Thus, the giant component of B is finite for all p values.

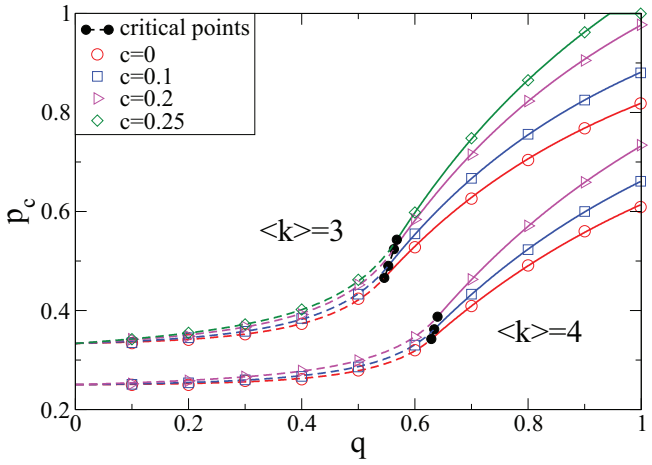

FIG. 2. (Color online) Percolation threshold, p_c, as a function of interdependency strength q ($q = q_A = q_B$) for $\langle k\rangle = \langle k\rangle_A = \langle k\rangle_B = 3$ and 4. Clustering coefficient c ($c = c_A = c_B$) ranges from 0 to 0.2 for $\langle k\rangle = 4$ and from 0 to 0.25 for $\langle k\rangle = 3$. For each $\langle k\rangle$ and c, there exists a critical point q_c (full circles). Above q_c, the system undergoes a first-order phase transition (solid lines) and below q_c, the system undergoes a second-order transition (dashed lines). Symbols represent simulation results and are in good agreement with theoretical predictions (solid and dashed lines). Note that for the same average degree $\langle k\rangle$, increasing clustering coefficient c increases p_c and yields a larger critical coupling, q_c.

results agree well with the theoretical results obtained from Eqs. (12). Note that, for strong coupling, as we increase the clustering coefficient the two interdependent networks become less robust. When the coupling is weak, the weakening effect of the clustering on the robustness is smaller. This can be seen in Fig. 2, which shows p_c versus $q = q_A = q_B$ for different clustering coefficients for both $\langle k\rangle = 3$ and $\langle k\rangle = 4$. Note that, for the same coupling strength q, a larger clustering coefficient yields a larger p_c, making the networks less robust. In addition, the critical coupling strength q_c below which the first-order phase transition changes to a second-order increases slightly as we increase clustering coefficient.

Figure 3 shows the size of the giant component in network A after each cascading step around the critical threshold for the first-order phase transition case [Fig. 3(a)] and the second-order phase transition case [Fig. 3(b)]. Note that the simulation results for the cascading failures agree well with analytical results (8) and (9). Different realizations give different results due to deviations from the mean field, rendering small fluctuations around the mean-field analytical results [58].

IV. NETWORK OF NETWORKS WITH CLUSTERING

The framework discussed above can also be generalized to an interdependent system consisting of more than two clustered networks. Here we consider two cases of NON [45–47] composed of n interdependent clustered networks, (i) a starlike NON and (ii) a random regular NON (see Fig. 4). We assume that for each pair of interdependent networks i and j ($i, j = 1, 2, \ldots, n$), there is a fraction q_{ji} of nodes in network i which depend on nodes in network j; i.e., they

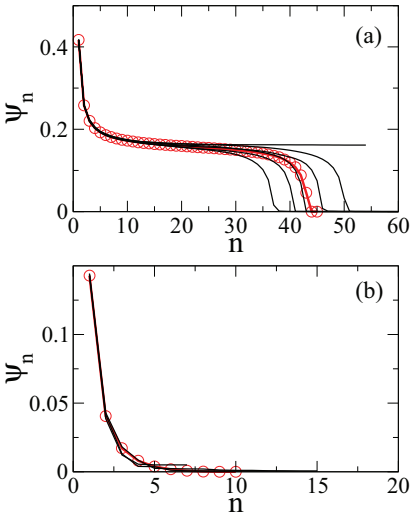

FIG. 3. (Color online) Size of the giant component in network A (ψ_n) as a function of cascading failure steps n for $\langle k\rangle = 4$, $c = 0.2$ for (a) $q = 0.8$ (first-order transition) and (b) $q = 0.6$ (second-order transition). The symbols (circles) and their connecting line are from the theoretical prediction. The other lines are several random realizations from simulations ($N = 10^6$). The value of $p = 0.569$ for (a) the first-order phase transition case and $p = 0.347$ for (b) the second-order phase transition case are both chosen to be just below critical thresholds obtained from theoretical predictions ($p_c = 0.57$ for the first-order case and $p_c = 0.3475$ for the second-order case). One can see that in both cases the agreement is very good. However, for first-order transition, after the plateau different realizations fluctuate.

cannot function if the nodes upon which they depend fail. Similarly, q_{ij} denotes the fraction of nodes in network j which depend on nodes in network i. We also assume here that a node from one network may depend on no more than one node from the other network and, if a node i in network A depends on a node j in network B and j depends on a node l in network A, then $l = i$ (a no-feedback condition). [45–47] After an initial attack, only a fraction p_i $(i = 1,2,\ldots,n)$ of nodes in each

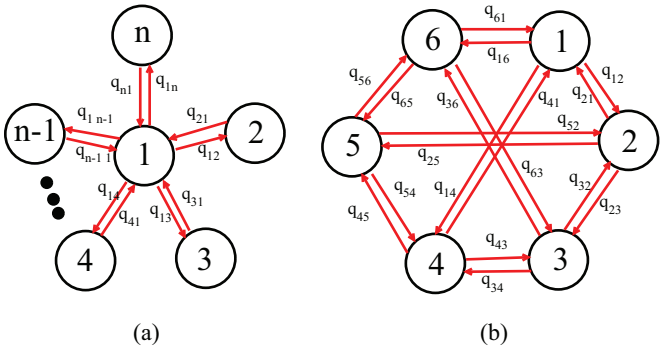

FIG. 4. (Color online) Schematic representation of two types of NONs: (a) Starlike NON where one central network is interdependent with $(n-1)$ other networks. (b) Random regular NON where each network depends exactly on m (here, $m = 3$) other networks. Circles represent interdependent networks and arrows represent interdependency relations. For example, q_{12} represents a fraction q_{12} of nodes in network 2 depend on nodes in network 1.

network will remain. After the period of cascading failures, a fraction $\psi_{\infty,i}$ of nodes in network i will remain functional. The final giant component of each network can be expressed as $\psi_{\infty,i} = x_i g_i(x_i)$ and the unknowns x_i can be found from a system of n equations [45–47],

$$x_i = p_i \prod_{j=1}^{K} [q_{ji} y_{ji} g_j(x_j) - q_{ji} + 1], \tag{14}$$

where the product is taken over the K networks that are coupled with network i. Since we consider the no-feedback condition [45–47], we have

$$y_{ji} = \frac{x_j}{q_{ij} y_{ij} g_i(x_i) - q_{ij} + 1}, \tag{15}$$

where y_{ji} is the fraction of nodes left in network j after it has suffered damage from all networks other than network i. We next consider two analytically solvable examples of a NON: a starlike network of ER networks and a random regular (RR) network of ER networks, shown in Fig. 4.

A. Starlike NON with clustering

For a starlike NON [Fig. 4(a)], we have a root network which is interdependent with other $(n-1)$ networks. For simplicity, the initial attack is on the root network, and a fraction $(1-p)$ of its nodes is removed. This damage spreads to the other networks and then returns to the root network, back and forth. Here we consider the case for n clustered ER networks with the same average degree $\langle k\rangle$ and the same clustering coefficient c (thus the same average number of triangles $\langle t\rangle$). Assuming, again for simplicity, that for all i, $q_{i1} = q_{1i} = q$, Eqs. (14) and (15) are simplified to two equations:

$$\begin{aligned} x_1 &= p[q g_2(x_2) - q + 1]^{n-1}, \\ x_2 &= pq g_1(x_1)[q g_2(x_2) - q + 1]^{n-2} - q + 1. \end{aligned} \tag{16}$$

For clustered ER networks, $f(x) = 1 - g(x)$ satisfies

$$f = \exp[\langle t\rangle x^2 (1-f)^2 - \langle k\rangle x(1-f)]. \tag{17}$$

By combining Eqs. (16) and (17), we find x_1, x_2 and f_1, f_2, from which the sizes of the giant components in the root network (ψ_∞) and in the other networks (ϕ_∞) can be obtained.

Figure 5 shows the size of the giant component in the root network for $n = 2$, 3, and 4 and compares two cases, $c = 0$ (no clustering) and $c = 0.2$ (high clustering). Note that the simulation results agree well with the theoretical predictions. Our results show that the NON becomes less robust with increasing n. For fixed n, the NON composed of networks with a larger clustering coefficient is less robust, and the effect of clustering in reducing the robustness becomes larger as n increases. Similarly, the critical coupling q_c, where the behavior of phase transition changes from first-order to second-order decreases with n and increases slightly with the clustering coefficient (see Fig. 6).

B. Random regular (RR) NON of ER networks with clustering

We now consider the case in which each clustered ER network depends on exactly m other clustered ER networks,

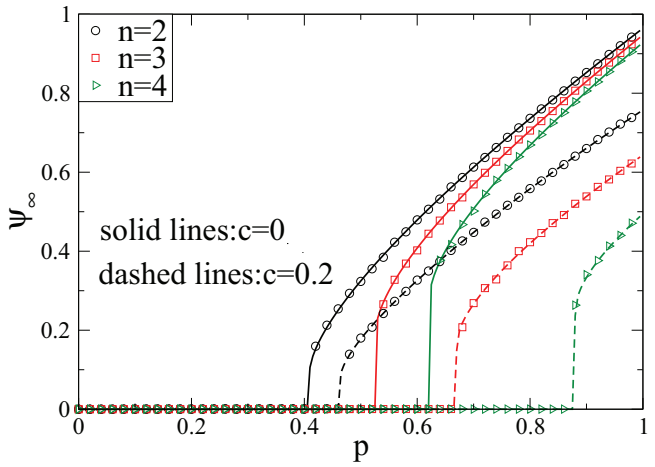

FIG. 5. (Color online) Size of the giant component in the root network as a function of p for $n = 2,3,4$ and $c = 0,0.2$ for starlike NON. Average degree of each network in the NON is $\langle k\rangle = 4$. Symbols and lines represent simulations ($N = 10^5$) and theory, respectively.

i.e., a random regular (RR) NON formed of clustered ER networks. Assume that the initial attack is on each network and randomly removes a fraction $(1 - p)$ of nodes and that the interacting strengths are all equal to q. Assume also that all ER networks have the same average degree $\langle k\rangle$ and the same average number of triangles $\langle t\rangle$. Because of symmetry, all equations in Eqs. (14) and Eqs. (15) are reduced into a single equation, and the size of the giant component in each network is

$$\psi_\infty = p(1 - e^{\langle t\rangle\psi_\infty^2 - \langle k\rangle\psi_\infty})\left[\frac{1-q+\sqrt{(1-q)^2+4q\psi_\infty}}{2}\right]^m. \tag{18}$$

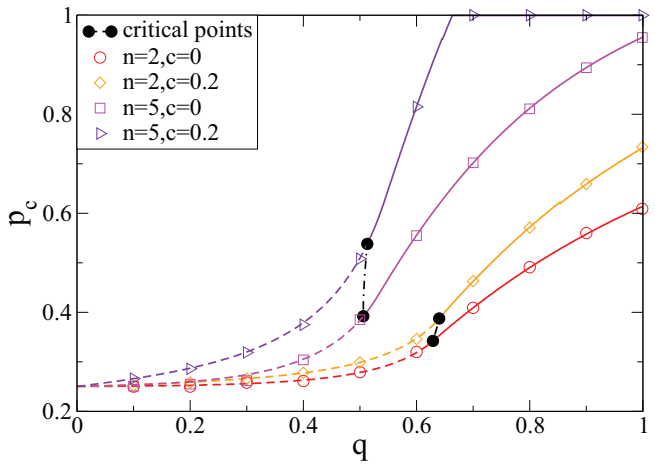

FIG. 6. (Color online) Critical threshold p_c as a function of interdependency strength, q, for clustered starlike NON for $\langle k\rangle = 4$, $n = 2,5$ and $c = 0,0.2$. For each n and c, there exists a critical interdependency strength q_c (solid symbols) that separates the first-order (solid lines) and second-order (dashed lines) phase transitions.

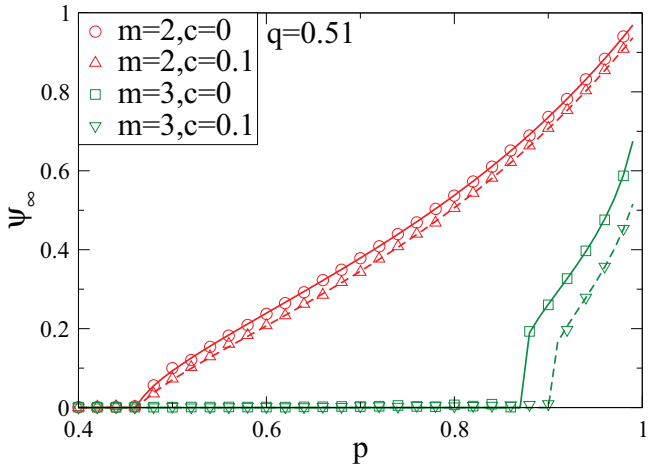

FIG. 7. (Color online) Size of the giant component, ψ_∞, as a function of p for RR NON of clustered ER networks for fixed q ($q = 0.51$). The average degree is $\langle k\rangle = 9$, $m = 2$, 3 and $c = 0$, 0.1. For $m = 3$, the system shows a first-order percolation transition as we change the value of p, while for $m = 2$, the phase transition is second-order.

Figures 7 and 8 show numerical solutions of Eq. (18) and simulation results. Note that the simulations agree well with theory. For a given $\langle k\rangle$, the size of the giant component ψ_∞ in each network displays a first- or a second-order phase transition as a function of p, depending on the values of q, m, and the clustering coefficient c. Figure 7 shows that, for some fixed values of $\langle k\rangle$ and q, the behavior of the phase transition can be either first-order or second-order for different values of m. Similarly, as shown in Fig. 8, for fixed values of $\langle k\rangle$ and m, different values of q can cause the phase transition to be first-order or second-order. In each scenario, when the transition is first-order the clustering within networks reduces the resistance of the NON to random node failure, but when

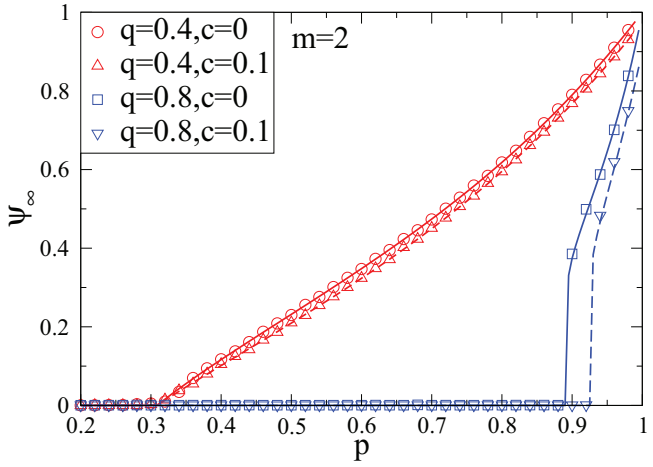

FIG. 8. (Color online) Size of giant component, ψ_∞, as a function of p for RR NON composed of clustered ER networks for fixed m ($m = 2$). The average degree is $\langle k\rangle = 9$, $q = 0.4$, 0.8 and $c = 0$, 0.1. The behavior of the phase transition is first-order for $q = 0.8$ and second-order for $q = 0.4$.

it is second-order the effect of clustering is similar but very small. This again is due to the smaller coupling value q in the second-order phase transition region. Note that for $q = 1$ and $m = 1$, the limit of two fully interdependent networks, Eq. (18) reduces to an equation similar to Eq. (16) in Huang *et al.* [51]. The only difference is because here we initially attack all networks, not just network A as in Ref. [51]. For $\langle t \rangle = 0$ (the no-clustering case), Eq. (18) reduces to Eq. (23) in Gao *et al.* [47].

By adding the condition that the first derivative of both sides of Eq. (18) with respect to ψ_∞ are equal, we obtain the critical threshold of the first-order phase transition, p_I. The critical threshold of the second-order phase transition p_{II} is solved by adding the condition $\psi_\infty(p_{II}) \to 0$ to Eq. (18). If we equate p_I and p_{II}, the critical coupling q_c where the first-order phase transition changes to a second-order phase transition can be derived analytically:

$$(\langle k \rangle^2 + 2\langle t \rangle)(1 - q_c)^2 = 2\langle k \rangle q_c m. \tag{19}$$

By substituting $c = \frac{2\langle t \rangle}{\langle k \rangle^2 + 2\langle t \rangle}$, we have

$$q_c = 1 + x - \sqrt{x(x+2)}, \tag{20}$$

where $x \equiv \frac{m}{\langle k \rangle}(1 - c)$. Note that increasing the clustering coefficient c increases the critical dependency q_c. Note also that for $c = 0$, Eq. (20) reduces to Eq. (30) of Ref. [47].

V. THE FIXED DEGREE DISTRIBUTION

The double-Poisson distribution model can display the features of clustering and it is possible to solve it analytically. Although in this model the average degree does not change, the degree distribution does change as the clustering coefficient changes. Here we consider another kind of joint distribution P_{st} proposed by Hackett *et al.* [52,59], which also preserves the total degree distribution $P(k)$ for different clustering coefficients. We set

$$P_{st} = P(k)\delta_{k,s+2t}[(1 - f)\delta_{t,0} + f\delta_{t,\lfloor (s+2t)/2 \rfloor}], \tag{21}$$

where $f \in [0,1]$ and $\lfloor . \rfloor$ is the floor function.

Equation (21) allows us to construct P_{st} from a given degree distribution $P(k)$ by picking a fraction f of nodes being attached to a maximum possible number of triangles while the remaining $(1 - f)$ nodes are attached to single edges only. From the definition of a clustering coefficient, we have

$$c = f\frac{\sum_k k[P(2k) + P(2k+1)]}{\sum_k \binom{k}{2} P(k)}; \tag{22}$$

hence the clustering coefficient can be adjusted by tuning the parameter f.

We investigate the effect of the joint degree distribution, Eq. (21), on the robustness of partially interdependent networks by comparing the two joint degree distributions. One is the fixed degree distribution (FDD), which is defined by Eq. (21) with $P(k)$ obeying a Poisson distribution ($P(k) = \langle k \rangle^k e^{-\langle k \rangle}/k!$). The other is the double-Poisson distribution (DPD) discussed in Sec. III, with $P_{st} = e^{-\langle s \rangle}\frac{\langle s \rangle^s}{s!}e^{-\langle t \rangle}\frac{\langle t \rangle^t}{t!}$.

Figure 9 plots the size of the giant component in network A for two partially interdependent networks with clustering. The joint degree distribution in each network is fixed as either FDD or DPD. The interdependent strength q is fixed as first-order. Note that the critical threshold p_c in FDD is larger than that in DPD when the clustering coefficient is the same. This difference in p_c is caused by the broadening of $P(k)$ in the double-Poisson distribution. Note that for site percolation on a single clustered network, a larger clustering coefficient leads to a higher critical threshold for both distributions [51,52]. For a system of two interdependent networks, the general trend is similar, and, for both degree distributions, p_c increases as the clustering coefficient increases. Figure 10 shows the size

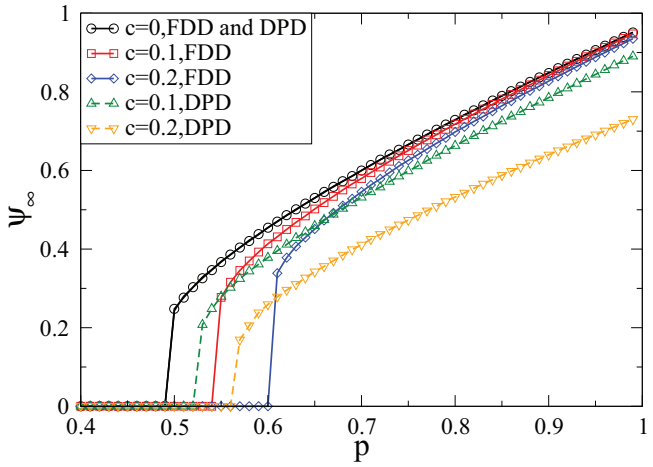

FIG. 9. (Color online) Size of giant component in network A for two partially interdependent networks with clustering. Circles, squares and diamonds represent results for a joint degree distribution which fix the total degree distribution being Poisson as we change the clustering coefficient (FDD). Circles, up-triangles, and down-triangles represent results for a double-Poisson distribution (DPD) with total average degree fixed. All resulted are from simulations with $N = 10^6$, $\langle k \rangle = 4$, and $q = 0.8 > q_c$. The behavior of the phase transition is first-order in both cases but p_c is larger for FDD.

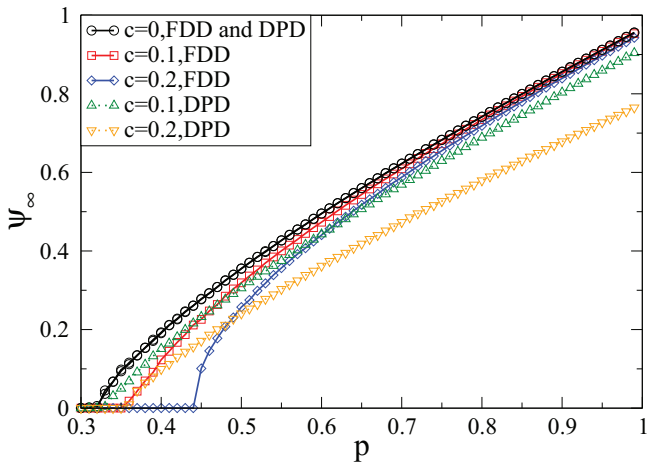

FIG. 10. (Color online) Size of giant component in network A for two partially interdependent networks with clustering. Circles, squares, and diamonds represent results for FDD, while circles, up-triangles, and down-triangles represent results for DPD. All results are from simulations with $N = 10^6$, $\langle k \rangle = 4$, and $q = 0.6 < q_c$. The behavior of the phase transition is second-order.

of the giant components in partially interdependent networks with a second-order phase transition for both FDD and DPD. The influence of clustering on the robustness of partially interdependent networks is larger for FDD than for DPD, but the general trend is similar in both distributions.

VI. CONCLUSIONS

We have developed a framework for studying percolation in a network formed of interdependent ER networks with clustering. For each clustering coefficient, the system shows a first-order to second-order transition as we decrease coupling strength q. As we increase the clustering coefficient of each network, the system becomes less robust. This influence of the clustering coefficient on network robustness decreases as we decrease the coupling strength, and the critical coupling strength q_c, at which the first-order phase transition changes to second-order, increases as we increase the clustering coefficient. We have also investigated the differences and similarities between two different joint degree distributions, FDD and DPD. We have found that, although the percolation threshold is different in the two cases, the general conclusion that an increase in the clustering coefficient causes interdependent networks to become less robust holds.

ACKNOWLEDGMENTS

We wish to thank ONR (Grant N00014-09-1-0380, Grant N00014-12-1-0548), DTRA (Grant HDTRA-1-10-1-0014, Grant HDTRA-1-09-1-0035), NSF (Grant CMMI 1125290), the European projects LINC, MULTIPLEX (EU-FET project 317532), and CONGAS (Grant FP7-ICT-2011-8-317672), the DFG, and the Israel Science Foundation for support.

[1] D. J. Watts and S. H. Strogatz, Nature (London) **393**, 440 (1998).
[2] R. Albert, H. Jeong, and A. L. Barabasi, Nature (London) **406**, 378 (2000).
[3] V. Rosato *et al*., Int. J. Crit. Infrastruct. **4**, 63 (2008).
[4] R. Albert and A. L. Barabasi, Rev. Mod. Phys. **74**, 47 (2002).
[5] R. Cohen, K. Erez, D. ben-Avraham, and S. Havlin, Phys. Rev. Lett. **85**, 4626 (2000); **86**, 3682 (2001).
[6] D. S. Callaway, M. E. J. Newman, S. H. Strogatz, and D. J. Watts, Phys. Rev. Lett. **85**, 5468 (2000).
[7] M. E. J. Newman, SIAM Rev. **45**, 167 (2003).
[8] S. N. Dorogovtsev and J. F. F. Mendes, *Evolution of Networks: From Biological Nets to the Internet and WWW (Physics)* (Oxford University Press, New York, 2003).
[9] C. Song *et al*., Nature (London) **433**, 392 (2005).
[10] G. Caldarelli and A. Vespignani, *Large Scale Structure and Dynamics of Complex Webs* (World Scientific, Singapore, 2007).
[11] R. Cohen and S. Havlin, *Complex Networks: Structure, Robustness and Function* (Cambridge University Press, Cambridge, 2010).
[12] M. E. J. Newman, *Networks: An Introduction* (Oxford University Press, New York, 2010).
[13] A. Bashan *et al*., Nature Commun. **3**, 702 (2012).
[14] G. Li, S. D. S. Reis, A. A. Moreira, S. Havlin, H. E. Stanley, and J. S. Andrade, Phys. Rev. Lett. **104**, 018701 (2010).
[15] C. M. Schneider, A. A. Moreira, J. S. Andrade, Jr., S. Havlin, and H. J. Herrmann, Proc. Natl. Acad. Sci. USA **108**, 3838 (2011).
[16] J. Ludescher, A. Gozolchiani, M. I. Bogachev, A. Bunde, S. Havlin, and H. J. Schellnhuber, Proc. Natl. Acad. Sci. USA **110**, 11742 (2013).
[17] X. Yan, Y. Fan, Z. Di, S. Havlin, and J. Wu, PLoS ONE **8**, e69745 (2013).
[18] S. Wasserman and K. Faust, *Social Network Analysis: Methods and Applications* (Cambridge University Press, Cambridge, 1994).
[19] E. Ravasz and A. L. Barabasi, Phys. Rev. E **67**, 026112 (2003).
[20] M. A. Serrano and M. Boguñá, Phys. Rev. E **74**, 056114 (2006).
[21] M. Boguñá and R. Pastor-Satorras, Phys. Rev. E **68**, 036112 (2003).
[22] E. M. Jin, M. Girvan, and M. E. J. Newman, Phys. Rev. E **64**, 046132 (2001).
[23] P. Holme and B. J. Kim, Phys. Rev. E **65**, 026107 (2002).
[24] K. Klemm and V. M. Eguiluz, Phys. Rev. E **65**, 036123 (2002).
[25] M. A. Serrano and M. Boguñá, Phys. Rev. E **72**, 036133 (2005).
[26] S. Bansal, S. Khandelwal, and L. A. Meyers, BCM Bioinformatics **10**, 405 (2009).
[27] M. E. J. Newman, Phys. Rev. Lett. **103**, 058701 (2009).
[28] S. V. Buldyrev, R. Parshani, G. Paul, H. E. Stanley, and S. Havlin, Nature (London) **464**, 1025 (2010).
[29] R. Parshani and S. V. Buldyrev, and S. Havlin, Phys. Rev. Lett. **105**, 048701 (2010).
[30] G. Dong, J. Gao, L. Tian, R. Du, and Y. He, Phys. Rev. E **85**, 016112 (2012).
[31] J. Shao, S. V. Buldyrev, S. Havlin, and H. E. Stanley, Phys. Rev. E **83**, 036116 (2011).
[32] A. Vespignani, Nature (London) **464**, 984 (2010).
[33] E. A. Leicht and R. M. D'Souza, arXiv:0907.0894 [cond-mat.dis-nn].
[34] R. G. Morris and M. Barthelemy, Phys. Rev. Lett. **109**, 128703 (2012).
[35] S.-W. Son *et al*., Europhys. Lett. **97**, 16006 (2012).
[36] A. Saumell-Mendiola, M. Á. Serrano, and M. Boguñá, Phys. Rev. E **86**, 026106 (2012).
[37] S. Gómez, A. Diaz-Guilera, J. Gomez-Gardenes, C. J. Perez-Vicente, Y. Moreno, and A. Arenas, Phys. Rev. Lett. **110**, 028701 (2013).
[38] J. Aguirre, D. Papo, and J. M. Buldú, Nature Phys. **9**, 230 (2013).
[39] C. D. Brummitt, R. M. D'Souza, and E. A. Leicht, Proc. Natl. Acad. Sci. USA **109**, 680 (2012).
[40] C. M. Schneider, N. Yazdani, N. A. M. Araújo, S. Havlin, and H. J. Herrmann, Sci. Rep. **3**, 1969 (2013).
[41] R. Parshani *et al*., Euro. Phys. Lett. **92**, 68002 (2010).
[42] Y. Hu, B. Ksherim, R. Cohen, and S. Havlin, Phys. Rev. E **84**, 066116 (2011).
[43] S. V. Buldyrev, N. W. Shere, and G. A. Cwilich, Phys. Rev. E **83**, 016112 (2011).
[44] A. Bashan, Y. Berezin, S. V. Buldyrev, and S. Havlin, Nature Phys. **9**, 667 (2013).
[45] J. Gao, S. V. Buldyrev, S. Havlin, and H. E. Stanley, Phys. Rev. Lett. **107**, 195701 (2011).
[46] J. Gao, S. V. Buldyrev, H. E. Stanley, and S. Havlin, Nature Phys. **8**, 40 (2012).

[47] J. Gao, S. V. Buldyrev, H. E. Stanley, X. Xu, and S. Havlin, Phys. Rev. E **88**, 062816 (2013).
[48] D. Cellai, E. López, J. Zhou, J. P. Gleeson, and G. Bianconi, Phys. Rev. E **88**, 052811 (2013).
[49] F. Radicchi and A. Arenas, Nature Phys. **9**, 717 (2013).
[50] M. De Domenico, A. Sole, S. Gomez, and A. Arenas, arXiv:1306.0519.
[51] X. Huang, S. Shao, H. Wang, S. V. Buldyrev, S. Havlin, and H. E. Stanley, Europhys. Lett. **101**, 18002 (2013).
[52] A. Hackett, S. Melnik, and J. P. Gleeson, Phys. Rev. E **83**, 056107 (2011).
[53] M. E. J. Newman, S. H. Strogatz, and D. J. Watts, Phys. Rev. E **64**, 026118 (2001).
[54] M. E. J. Newman, Phys. Rev. E **66**, 016128 (2002).
[55] P. Erdős and A. Rényi, Publ. Math. **6**, 290 (1959).
[56] P. Erdős and A. Rényi, Inst. Hung. Acad. Sci. **5**, 17 (1960).
[57] B. Bollobás, *Random Graphs* (Academic, London, 1985).
[58] D. Zhou, A. Bashan, Y. Berezin, R. Cohen, and S. Havlin, arXiv:1211.2300 (2012).
[59] J. P. Gleeson, S. Melnik, and A. Hackett, Phys. Rev. E **81**, 066114 (2010).